Features of $\pi\Delta$ Photoproduction at High Energies

J. Nys[a,b,c,d,e,*], V. Mathieu[d], A. Szczepaniak[b,c,d], J. Ryckebusch[a], G. Fox[f],

(Joint Physics Analysis Center)

[a] *Department of Physics and Astronomy, Ghent University, B-9000 Ghent, Belgium*
[b] *Physics Department, Indiana University, Bloomington, IN 47405, USA*
[c] *Center for Exploration of Energy and Matter, Indiana University, Bloomington, IN 47403, USA*
[d] *Theory Center, Thomas Jefferson National Accelerator Facility, Newport News, VA 23606, USA*
[e] *The George Washington University, Washington, DC 20052, USA*
[f] *School of Informatics, Computing, and Engineering, Indiana University, Bloomington, IN 47405, USA*

Abstract

We study $\pi\Delta$ photoproduction at high energies $5 \leq E_{\text{lab}} \leq 16$ GeV. We provide predictions for the beam asymmetry at Jefferson Lab energies of $E_{\text{lab}} = 9$ GeV.

Keywords:
PACS: JLAB-THY-

1. Intro

There is mounting evidence for the existence of exotic hadrons that cannot be accommodated within the conventional quark model [1]. Specifically, light flavor hybrid mesons are expected to appear in the spectrum below 2 GeV [2, 3] and to be copiously produced via beam fragmentation in peripheral photoproduction, with photon energies on the order of 10 GeV [4–6]. Experiments dedicated to exploration of the hybrid meson spectrum have just begun using GlueX and CLAS12 detectors at Jefferson Lab. The success of these experiments relies on accurate theoretical description of both production and decay characteristics of resonances in peripheral photoproduction [7]. While resonance decays have been extensively studied in recent years, in view of the forthcoming data, efforts aiming at constraining production mechanisms need to be revisited [8–11]. Photoproduction of the light exotic mesons involves the same, natural ($P(-1)^J = 1$) and unnatural ($P(-1)^J = -1$) parity Regge exchanges that determine photoproduction of pseudoscalar mesons. The aforementioned experiments have begun a systematic study of pion and η meson production with the goal of establishing the production mechanisms [12–15]. Understanding of pion exchange is of particular interest since virtual pions play an important role in various hadronic process, inclusive possibly being involved in formation of hadron molecules [16, 17]. In peripheral production, pion exchange dominates forward production and by being the lightest, it is also sensitive to absorption dynamics *i.e.* final states interactions [18]. In this context the beam asymmetry in charged pion photoproduction is an important observable as it can be used to disentangle the parity of the exchanged Reggeons and thus to identify the contribution from pion exchanges. In this

*Corresponding author
Email address: jannes.nys@ugent.be (J. Nys)

work we give a theoretical prediction for the beam asymmetry, Σ in charged pion photoproduction associated with production of the Δ excitation from the proton target. The asymmetry in this reaction is expected to be soon determined in the GlueX and CLAS12 measurements. Previous attempts have been made to describe the high-energy observables. These models either fail or do not attempt to reproduce both the complicated energy and t dependence [8, 19, 20] and the aim of this work is to give a proper account of these dependencies in the kinematic region relevant to the JLab experiments.

2. Model

At low momentum transfer, $\pi\Delta$ photoproduction is dominated by pion exchange. At photon energies in tens of GeV's and/or $-t \simeq 0.5$ GeV^2 it is expected to be dominated by natural, vector, ρ and tensor, a_2 exchanges. There is also a contribution from the unnatural, b exchange. In the Regge pole approximation the asymptotic expression ($s \to \infty$) of the s-channel helicity amplitude describing the reaction $1+2 \to 3+4$ is given by [18, 21, 22]

$$A^R_{\mu_4\mu_3,\mu_2\mu_1} = \beta^R_{\mu_1\mu_2\mu_3\mu_4}(t)\mathcal{P}_R(s,t). \tag{1}$$

Here μ_i are the s-channel helicities and $\mathcal{P}_R(s,t)$ is the Regge propagator,

$$\mathcal{P}_R = \frac{\pi\alpha_1^R}{2}\frac{\tau_R + e^{-i\pi\alpha^R(t)}}{\sin\pi\alpha^R(t)}\left(\frac{s}{s_0}\right)^{\alpha^R(t)} \tag{2}$$

with τ_R and α_1^R being the signature and slope of the Regge trajectory, respectively. The $s_0 = 1$ GeV^2 is a scale factor. From unitarity it follows that the residues $\beta^R_{\mu_1\mu_2\mu_3\mu_4}(t)$ are factorizable, *i.e.* $\beta^R_{\mu_1\mu_2\mu_3\mu_4}(t) = \beta^{R,13}_{\mu_1\mu_3}(t)\beta^{R,24}_{\mu_2\mu_4}(t)$. Angular-momentum and parity conservation determine the non-analytical dependence on t, $\beta^{R,ij}_{\mu_i\mu_j}(t) = \sqrt{-t}^{|\mu_i-\mu_j|}\hat{\beta}^{R,ij}_{\mu_i\mu_j}(t)$ where the reduced residues, $\hat{\beta}^{R,ij}_{\mu_i\mu_j}(t)$ are regular in t [23]. In the case at hand, $\beta^R_{\mu_\gamma\mu_N\mu_\Delta}(t) = \beta^{R,\gamma\pi}_{\mu_\gamma}(t)\beta^{R,N\Delta}_{\mu_N\mu_\Delta}(t)$ with $\beta^{R,\gamma\pi}_{\mu_\gamma}(t) \propto \sqrt{-t}$. That is, in the Regge pole approximation the helicity amplitudes in the photon vertex for pion production vanish near $t=0$. From overall angular momentum conservation it follows, however, that the s-channel helicity amplitude is proportional to the half-angle factor $\xi_{\mu\mu'}(s,t) = (s(1-z_s)/2)^{|\mu-\mu'|}((1+z_s)/2)^{|\mu+\mu'|}$ where $\mu = \mu_1 - \mu_2$ and $\mu' = \mu_3 - \mu_4$ is the net helicity flip in the initial and final state, respectively. This term incorporates the kinematic singularity in t, and it asymptotically reduces to $\sqrt{-t}^{|\mu-\mu'|}$. Matching with the Regge pole form in the asymptotic amplitude given in Eq. (1), one finds [21]

$$A^R_{\mu_4\mu_3,\mu_2\mu_1} = \xi_{\mu\mu'}(s,t)\sqrt{-t}^{-|\mu-\mu'|}\left[\beta^R_{\mu_1\mu_2\mu_3\mu_4}(t)\mathcal{P}_R(s,t)\right] \tag{3}$$

The residual, analytical dependence on t is not predicted by the Regge theory alone and in the following, we use the single-particle exchange model and the data as guidance. Specifically, if e represents the lightest meson on the trajectory R, one expects that for small momentum transfer $\hat{\beta}^{R,ij}(t) \approx \hat{\beta}^{e,ij}(t)$, since the Regge and particle exchange residues must be equal at the pole $t \to m_e^2$. The residues $\hat{\beta}^{e,ij}(t)$ are proportional to constant couplings $g_{e,ij}$ in an effective Lagrangian (see Table 3) and the single-meson exchange amplitude in the $s \to \infty$ limit have the form given by,

$$A^e_{\mu_\Delta,\mu_N\mu_\gamma} = \sqrt{-t}^{|\mu_\gamma|}\sqrt{-t}^{|\mu_N-\mu_\Delta|}\hat{\beta}^{e,N\Delta}_{\mu_N\mu_\Delta}(t)\hat{\beta}^{e,\gamma\pi}_{\mu_\gamma}(t)\mathcal{P}_e(s,t)\,, \tag{4}$$

where $\mathcal{P}_e = (s/s_0)^{J_e}/(m_e^2 - t)$ is the exchange particle propagator. The Regge propagator in Eq. (2) is normalized such that for $t \to m_e^2$, $\mathcal{P}_R \to \mathcal{P}_e$. By comparing with Eq. (3) one determines the relation between the reduced Regge residues and the elementary couplings, which is summarized in Table 3. Besides pion exchanges, in the following we include the ρ, a_2 and b exchanges with signatures, $\tau_{\pi,a_2} = +1$ and $\tau_{\rho,b} = -1$, respectively. We use coupling constants extracted from the corresponding decay widths, as shown in Table 1 and assume degenerate ρ and a_2 trajectories, $\alpha^N \equiv \alpha^{R=\rho,a_2}(t) = 0.9(t - m_\rho^2) + 1$, while for the unnatural π and b exchanges we use $\alpha^U \equiv \alpha^{R=\pi,b}(t) = 0.7(t - m_\pi^2)$. The pion exchange is known to be strongly affected by absorption [18], which can be effectively accounted for by a simple modification of Regge pole amplitude, known as the 'William's poor man absorption model' (PMA) [24]. In PMA the $\sqrt{-t}$ factors in the residues that are required by factorization but not by the overall angular momentum conservation are evaluated at the pion pole. Although different in the underlying physics assumptions, in practice, PMA approximation is equivalent to a model in which an s-channel electric Born term is added to t-channel pion exchange [25, 26]. We analyze the differential cross section, beam asymmetry and the differential cross section for photons polarized parallel and perpendicular to the reaction plane for $\gamma p \to \pi^- \Delta^{++}$ and $\gamma p \to \pi^+ \Delta^0$ [27, 28]. In terms of the helicity amplitudes these are given by

$$\frac{\mathrm{d}\sigma}{\mathrm{d}t} = \frac{K}{4} \sum_{\mu_\Delta,\mu_N,\mu_\gamma} |A_{\mu_\Delta,\mu_N\mu_\gamma}|^2, \tag{5}$$

$$\Sigma\frac{\mathrm{d}\sigma}{\mathrm{d}t} = \frac{K}{4} \sum_{\mu_\Delta,\mu_N} 2\,\mathrm{Re}\, A_{\mu_\Delta,\mu_N\mu_\gamma=+1} A^*_{\mu_\Delta,\mu_N\mu_\gamma=-1}, \tag{6}$$

$$\frac{\mathrm{d}\sigma_{\perp/\parallel}}{\mathrm{d}t} = \frac{K}{4} \sum_{\mu_\Delta,\mu_N} |A_{\mu_\Delta,\mu_N\mu_\gamma=+1} \pm A_{\mu_\Delta,\mu_N\mu_\gamma=-1}|^2, \tag{7}$$

with $K = (64\pi s p_{s12}^2)^{-1}$. In the first step we extract the effective trajectory $\alpha_{\text{eff}}(t)$ from the energy dependence of the differential cross section, see Fig. 1. As expected, we find that pion exchange $\alpha_{\text{eff}} \simeq 0$ dominates at small $-t$, while natural exchange contributions become important at $-t \geq 0.5$ GeV^2 resulting in $\alpha_{\text{eff}}(t) \simeq 0.5$. Overall, however, $\alpha_{\text{eff}}(t)$ is not as steep as compared to the expectation from a pure Regge pole indicating presence Reggeon-Pomeron interference or daughter poles, which in general flatten the t dependence. Guided by this observation consider two scenarios. In one, the ρ and a_2 exchanges are described as pure Regge poles and in the other we include final state interaction corrections. In the later case we simply replace the pole trajectory by, $\alpha^N(t) \to \alpha^C(t) = \alpha_0^N + \alpha_0^{\mathbb{P}} - 1 + t(\alpha_1^N \alpha_1^{\mathbb{P}})/(\alpha_1^N + \alpha_1^{\mathbb{P}})$. Here, $\alpha_0^{N,\mathbb{P}}$ and $\alpha_1^{N,\mathbb{P}}$ are the intercepts and slopes of the natural Regge pole and the Pomeron trajectory. For the latter we use $\alpha^{\mathbb{P}}(t) = 1.08 + 0.25t$ [29]. In addition the amplitude is multiplied be a factor $(\ln s/s_0)^{-1}$ [18]. Even though the cut trajectory and effective trajectory do not fully match (see Fig. 1), the remaining factors in the Regge amplitude, *i.e* the half-angle factor and the extra $\ln s/s_0$ dependence ultimately results in a good agreement with the data (see Fig. 2). While in the Regge-Pomeron cut model for the ρ and a_2, the connection between the Regge and single-particle residues is lost, we still apply the same parametrization since it provides enough freedom in the fit. It has been verified that alternative parameterizations for the t-dependence of the residues of the natural exchanges do not change the conclusions of the following analysis, nor do they significantly alter the predictions for JLab energies.

The Regge propagator in Eq. (2) contains ghost poles which must be canceled by zeros in the residues. Exchange degeneracy (EXD) forces these zeros to be present in the residue of the

EXD partner as well, implying zeros in the amplitude. The latter are referred to as nonsense wrong-signature zeros (NWSZ). Since EXD does not in general hold for the overall residue in photoproduction reactions, we only remove those ghost poles for each individual Reggeon that are closest to the physical region under consideration, without including NWSZ. In particular, we only remove the ghost poles[1] at spins, $\alpha = -2$ for π, $\alpha = -1$ for b, $\alpha = -1$ for ρ and $\alpha = 0$ and $\alpha = -2$ for the a_2. The unnatural and natural contributions have an overall exponential factor which accounts for the phenomenological falloff at large values of $-t$. Explicitly,

$$\hat{\beta}^{R=\pi}_{\mu_\gamma \mu_N \mu_\Delta}(t) = g_\pi \hat{\beta}^{e=\pi}_{\mu_\gamma \mu_N \mu_\Delta}(t) e^{b_U t}(\alpha+2)/2 \tag{8}$$

$$\hat{\beta}^{R=b}_{\mu_\gamma \mu_N \mu_\Delta}(t) = g_\pi \hat{\beta}^{e=b}_{\mu_\gamma \mu_N \mu_\Delta}(t) e^{b_U t}(\alpha+1) \tag{9}$$

$$\hat{\beta}^{R=\rho}_{\mu_\gamma \mu_N \mu_\Delta}(t) = \hat{\beta}^{e=\rho}_{\mu_\gamma \mu_N \mu_\Delta}(t) e^{b_N t}(\alpha+1)/2 \tag{10}$$

$$\hat{\beta}^{R=a_2}_{\mu_\gamma \mu_N \mu_\Delta}(t) = \hat{\beta}^{e=a_2}_{\mu_\gamma \mu_N \mu_\Delta}(t) e^{b_N t}\alpha(\alpha+2)/3 \tag{11}$$

The $\hat{\beta}$ on the left and right hand side of the above equations are the Regge and single-particle residues respectively. We introduced an additional factor g_π in order to allow small deviations from the estimated pion couplings. We require $\hat{\beta}^{a_2,p\Delta^{++}}(t) = \sqrt{s_0}\hat{\beta}^{\rho p\Delta^{++}}(t)$ and $\hat{\beta}^{bp\Delta^{++}}(t) = \sqrt{s_0}\hat{\beta}^{\pi p\Delta^{++}}(t)$ up to the ghost killing factors. For the photon vertex we use the radiative decay couplings from Table 1. At this point, it is worth mentioning that NWSZ are not favored by the data. Absence of such zeros was noted in the analysis of Yu *et al.* [8], where to fill in the dips, the authors replace the signature factors of the ρ and a_2 with a different phase. While the physics behind such a phase is not well justified in principle[2], the effect of this substitution is to remove the NWSZ in both contributions. Finally we note that two $\pi\Delta$ channels are related by isospin, (neglecting isospin 2)

$$A(\gamma p \to \pi^+ \Delta^0) = (A^+ + A^-)/\sqrt{3} \tag{12}$$

$$A(\gamma p \to \pi^- \Delta^{++}) = A^+ - A^- \tag{13}$$

where the A^G (G is the t-channel G-parity) receive contributions from ρ and b, $A^+ = A^\rho + A^b$ and a_2 and π, $A^- = A^{a_2} + A^\pi$, respectively.

3. Results

The available data set includes the differential cross sections, polarization cross sections and beam asymmetries at a single energy $E_{\text{lab}} = 16$ GeV for the two isospin channels $\pi^+\Delta^0$ and $\pi^-\Delta^{++}$. High-energy data at other energies in the range $5 \leq E_{\text{lab}} \leq 16$ GeV are available for $\pi^-\Delta^{++}$ only. For definite parity exchanges, the polarization cross sections are useful, since they are sensitive to a given naturality in the t-channel. Specifically, $d\sigma_\perp$ ($d\sigma_\parallel$) are determined by natural (unnatural) contributions [13], respectively, thus $d\sigma_\parallel$ allows to study π exchange in isolation. It should be noted, however, that absorption effectively changes the naturality of the π exchange and PMA specifically results, in the forward region, in an equal contribution to both naturalities.

[1] In removing these ghost poles we respect the normalization of the residues on the lightest mass pole of the EXD trajectories.

[2] EXD is an equality between two Reggeons. The constant and rotating phases are in principle obtained when two Regge contributions with equal residues are added or subtracted.

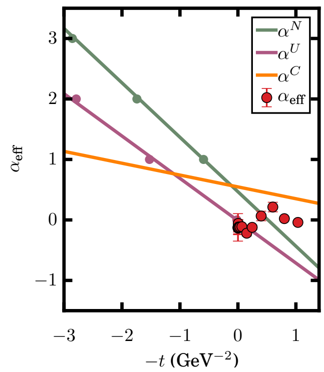

Figure 1: Effective trajectory of the cross section, $\alpha_{\rm eff}(t)$ extracted using in $\mathrm{d}\sigma/dt = f(t)s^{2\alpha_{\rm eff}(t)-2}$ (red). The green and purple solid curves illustrate the Regge trajectories used in this work, together with observed particles. The orange line depicts the $\rho \otimes \mathbb{P}$ or $a_2 \otimes \mathbb{P}$ cut trajectory.

From the analysis of radiative decays and Table 3, we find $\beta^{a_2\pi\gamma}/\beta^{\rho\pi\gamma} = 1.82$ and $\beta^{\pi\pi\gamma}/\beta^{b\pi\gamma} = 4.38$. Hence, the ρ and b contributions are suppressed with respect to their opposite signature partners. In Refs. [19] the authors used the average value of 3 both ratios. The obtained g_π value is consistent with unity and is mainly fixed by the $\mathrm{d}\sigma_\parallel$ data, which is dominated by π exchange. Observing a significant difference in $\mathrm{d}\sigma_\perp$ between the two isospin channels in the region around $\sqrt{-t} = 0.4$ GeV, one concludes that the ρ and a_2 contributions must have a rather strong t-dependence. Indeed, one can exclude the presence of strong variations in t in the pion residue due to the rather featureless t dependence of $\mathrm{d}\sigma_\parallel$. Since the $\rho N\Delta$ couplings are not well constrained, we obtain them from a fit. The PMA model reproduces well the forward behavior, thereby correctly matching the natural and unnatural contributions. Indeed, all natural contributions stemming from ρ and a_2 exchanges are suppressed in the forward direction by the $\sqrt{-t}$ factors. By neglecting the b exchange contribution, the difference between the isospin channels is attributed to the interference of the a_2 with the ρ and π terms. If the ρ exchange has a NWSZ at $t = -0.55$ GeV^2, $A^+ \approx 0$ and the two isospin channels would coincide in this region. This is not observed in the data. Hence, the residues of ρ cannot contain NWSZ within the pure Regge pole model. The NWSZ in the $\pi^+p \to \pi^0\Delta^{++}$ cross section must therefore be accounted for by the $\rho\pi\pi$ residue. A similar lack of NWSZ in the ρ exchange in photoproduction reactions was found in Ref. [14], where a detailed mapping of the t-dependence of the residues was carried out through the use of finite-energy sum rules.

The fits are constrained to all the available $E_{\rm lab} = 16$ GeV data, leaving the $E_{\rm lab} = 5, 8, 11$ GeV cross section data as a prediction and model validation. The results of the fits are shown in Fig. 2. The fitted parameters are given in Table 2. Even though both the pure pole and pole-plus-cut model describe the data rather well, we observe quite a sensitivity in the normalization of the $\rho N\Delta$ couplings. Thus an independent estimate of these parameters, would be very important. In our fits this is driven by the large difference in the observed beam asymmetry for the two isospin channels. The model in Ref. [8] was not given as much freedom in a fit to the data as in the current analysis, but rather the couplings were constrained by symmetry arguments. However, from a comparison of the presented model with the one in Ref. [8], it becomes clear that pure pole-like contributions with natural size couplings are not able to reproduce this behavior. The new experiments at JLab will be able to address this complex feature. The main deficiency of the poles-only fit is that it overestimates the s-dependence of the $\pi^-\Delta^{++}$ cross section at large $-t$. A natural-parity cut contribution coincides with the observed energy dependence, except for the $E_{\text{lab}} = 5$ GeV data. At such low energies, daughter and additional cut contributions are expected.

We give predictions for the beam asymmetry at JLab energies of $E_{\text{lab}} = 9$ GeV. The predicted observable appears rather similar to the SLAC data at $E_{\text{lab}} = 16$ GeV [30]. The underlying dynamics can be interpreted in the following way. At high $-t$, $\Sigma \approx +1$ indicates dominance of natural exchanges. As $-t$ becomes smaller, pion exchanges dominate the forward region, which is reflected by $\Sigma \to -1$. For $t' \to 0$, one expects $\Sigma = -1$ for purely factorizable exchanges, since the pion remains the dominant contribution up to extremely forward angles. However, the effect of $\Sigma \to 0$ indicates the presence of additional non-pole terms of equal parity in the t-channel, as successfully included by the PMA model.

Table 1: Decay widths [31] and respective couplings. Normalizations of the couplings are consistent with Table 3.

Expression $\Gamma(g)$	Γ	g
$\Gamma_{\rho^\pm \to \pi^\pm \gamma} = g^2_{\rho\pi\gamma} p^3/(12\pi m^2_\rho)$	68 keV	$g_{\rho\pi\gamma} = 0.17$
$\Gamma_{b_1^\pm \to \pi^\pm \gamma} = g^2_{b_1\pi\gamma} p^3/(12\pi m^2_{b_1})$	230 keV	$g_{b_1\pi\gamma} = 0.24$
$\Gamma_{a_2^\pm \to \pi^\pm \gamma} = g^2_{a_2\pi\gamma} p^5/(20\pi m^4_{a_2})$	311 keV	$g_{a_2\pi\gamma} = 0.71$
$\Gamma_{\Delta \to \pi N} = g^2_{\pi\Delta N} p^3(m_N + \sqrt{p^2 + m^2_N})/(12\pi m^3_\Delta)$	116 MeV	$g_{\pi\Delta N} = 19.16$

Table 2: Fitted parameters for the two models.

	Pole model	Cut model
g_π	1.06	1.04
$b_U(\text{GeV}^{-2})$	0.06	0.14
$b_N(\text{GeV}^{-2})$	−0.42	−2.12
$g^{(1)}_{\rho N\Delta}$	−48.2	−370.8
$g^{(2)}_{\rho N\Delta}$	−52.4	−242.4
$g^{(3)}_{\rho N\Delta}$	40.2	−139.0

Acknowledgement

This material is based upon work supported in part by the Research Foundation Flanders (FWO-Flanders), the U.S. Department of Energy, Office of Science, Office of Nuclear Physics under contract DE-AC05-06OR23177. This work was also supported in part by the U.S. Department of Energy under Grant DE-FG0287ER40365, National Science Foundation under Grants PHY-1415459 and PHY-1205019, the IU Collaborative Research Grant.

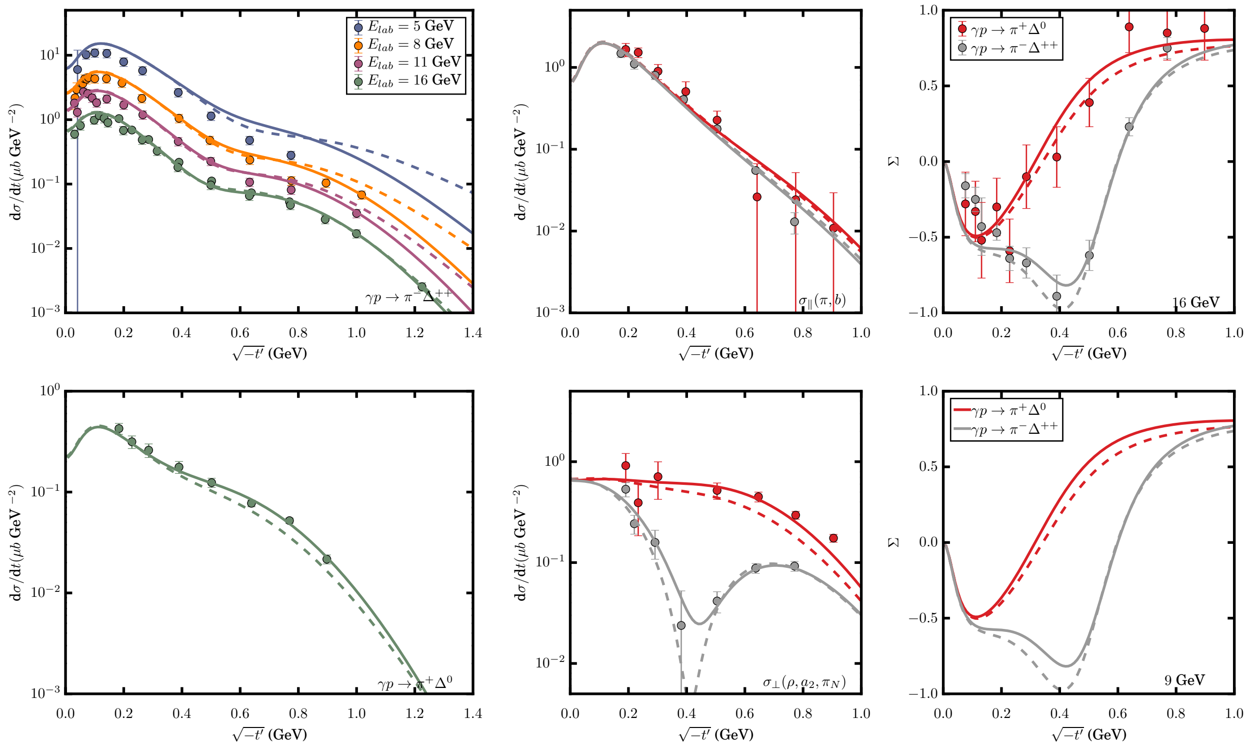

Figure 2: The comparison of pole (dashed) and cut (solid) models with the available (unpolarized) differential cross section and beam asymmetry data from Refs.[27, 28, 30]. We also show the predictions for $p_{\text{lab}} = 9$ GeV which is relevant for the GlueX experiment. The data and model for $\gamma p \to \pi^- \Delta^0$ have been rescaled by a factor of 3 to compensate the overall isospin coefficient in Eq. (12).

[1] C. A. Meyer and E. S. Swanson, Prog.Part.Nucl.Phys. **82**, 21 (2015), arXiv:1502.07276 [hep-ph] .
[2] J. J. Dudek, Phys.Rev. **D84**, 074023 (2011), arXiv:1106.5515 [hep-ph] .
[3] J. J. Dudek, R. G. Edwards, P. Guo, and C. E. Thomas (Hadron Spectrum), Phys.Rev. **D88**, 094505 (2013), arXiv:1309.2608 [hep-lat] .
[4] F. E. Close and P. R. Page, Phys.Rev. **D52**, 1706 (1995), arXiv:hep-ph/9412301 [hep-ph] .
[5] A. V. Afanasev and A. P. Szczepaniak, Phys.Rev. **D61**, 114008 (2000), arXiv:hep-ph/9910268 [hep-ph] .
[6] A. P. Szczepaniak and M. Swat, Phys.Lett. **B516**, 72 (2001), arXiv:hep-ph/0105329 [hep-ph] .
[7] M. Battaglieri *et al.*, Acta Phys.Polon. **B46**, 257 (2015), arXiv:1412.6393 [hep-ph] .
[8] B.-G. Yu and K.-J. Kong, Phys. Lett. **B769**, 262 (2017), arXiv:1611.09629 [hep-ph] .
[9] V. L. Kashevarov, M. Ostrick, and L. Tiator, Phys.Rev. **C96**, 035207 (2017), arXiv:1706.07376 [hep-ph] .
[10] B. G. Yu, T. K. Choi, and W. Kim, Phys. Rev. **C83**, 025208 (2011), arXiv:1103.1203 [nucl-th] .
[11] B.-G. Yu and K.-J. Kong, (2017), arXiv:1710.04511 [hep-ph] .
[12] H. Al Ghoul *et al.* (GlueX), Phys.Rev. **C95**, 042201 (2017), arXiv:1701.08123 [nucl-ex] .
[13] V. Mathieu, G. Fox, and A. P. Szczepaniak, Phys.Rev. **D92**, 074013 (2015), arXiv:1505.02321 [hep-ph] .
[14] J. Nys, V. Mathieu, C. Fernndez-Ramrez, A. N. Hiller Blin, A. Jackura, M. Mikhasenko, A. Pilloni, A. P. Szczepaniak, G. Fox, and J. Ryckebusch (JPAC), Phys.Rev. **D95**, 034014 (2017), arXiv:1611.04658 [hep-ph] .
[15] V. Mathieu, J. Nys, C. Fernndez-Ramrez, A. Jackura, M. Mikhasenko, A. Pilloni, A. P. Szczepaniak, and G. Fox, (2017), arXiv:1704.07684 [hep-ph] .
[16] F.-K. Guo, C. Hanhart, U.-G. Meißner, Q. Wang, Q. Zhao, and B.-S. Zou, “Hadronic molecules,” (2017), arXiv:1705.00141 [hep-ph] .
[17] T. E. O. Ericson and G. Karl, Phys. Lett. **B309**, 426 (1993).
[18] A. C. Irving and R. P. Worden, Phys.Rept. **34**, 117 (1977).
[19] G. R. Goldstein and J. F. Owens, Nucl.cPhys. **B71**, 461 (1974).

Table 3: The s-channel residues from single-meson exchange terms (up to isospin Clebsches). These are obtained by using the Lagrangians in Refs. [8, 10, 32–35]. All residues must be multiplied by a factor $\sqrt{s_0}^{J_e}$ where J_e is the spin of the corresponding exchange e.

$\hat{\beta}^{e,if}_{\mu_i\mu_f}$	Expression
$\hat{\beta}^{\pi,\gamma\pi}_{+1}(t)$	$\sqrt{2}e$
$\hat{\beta}^{\rho,\gamma\pi}_{+1}(t)$	$\frac{g_{\rho\pi\gamma}}{2m_\rho}$
$\hat{\beta}^{b_1,\gamma\pi}_{+1}(t)$	$\frac{g_{b_1\pi\gamma}}{2m_{b_1}}$
$\hat{\beta}^{a_2,\gamma\pi}_{+1}(t)$	$\frac{g_{a_2\pi\gamma}}{2m_{a_2}^2}$
$\hat{\beta}^{\pi,N\Delta}_{+\frac{1}{2}+\frac{3}{2}}(t)$	$\frac{g_{\pi\Delta N}(m_N+m_\Delta)}{\sqrt{2}m_\Delta}$
$\hat{\beta}^{\pi,N\Delta}_{-\frac{1}{2}+\frac{1}{2}}(t)$	$\frac{g_{\pi\Delta N}(-m_N^2+m_N m_\Delta+2m_\Delta^2+t)}{\sqrt{6}m_\Delta^2}$
$\hat{\beta}^{\pi,N\Delta}_{+\frac{1}{2}+\frac{1}{2}}(t)$	$\frac{-g_{\pi\Delta N}(-m_N^3-m_N^2 m_\Delta+m_\Delta^3+2m_\Delta t+m_N(m_\Delta^2+t))}{\sqrt{6}m_\Delta^2}$
$\hat{\beta}^{\pi,N\Delta}_{-\frac{1}{2}+\frac{3}{2}}(t)$	$\frac{-g_{\pi\Delta N}}{\sqrt{2}m_\Delta}$
$\hat{\beta}^{\rho,N\Delta}_{+\frac{1}{2}+\frac{3}{2}}(t)$	$\frac{-(2m_\Delta g^{(1)}_{\rho N\Delta}+g^{(2)}_{\rho N\Delta}(m_N-m_\Delta))}{2m_\Delta^2}$
$\hat{\beta}^{\rho,N\Delta}_{-\frac{1}{2}+\frac{1}{2}}(t)$	$\frac{-(2m_N m_\Delta g^{(1)}_{\rho N\Delta}+g^{(2)}_{\rho N\Delta}(-m_N m_\Delta+m_\Delta^2+2t)+2tg^{(3)}_{\rho N\Delta})}{2\sqrt{3}m_\Delta^3}$
$\hat{\beta}^{\rho,N\Delta}_{+\frac{1}{2}+\frac{1}{2}}(t)$	$\frac{-(2m_\Delta g^{(1)}_{\rho N\Delta}+g^{(2)}_{\rho N\Delta}(2m_N-3m_\Delta)+2g^{(3)}_{\rho N\Delta}(m_N-m_\Delta))}{2\sqrt{3}m_\Delta^3}(-t)$
$\hat{\beta}^{\rho,N\Delta}_{-\frac{1}{2}+\frac{3}{2}}(t)$	$\frac{g^{(2)}_{\rho N\Delta}}{2m_\Delta^2}$

[20] R. B. Clark, Phys.Rev. **D18**, 1444 (1978).
[21] P. D. B. Collins, Phys.Rept. **1**, 103 (1971).
[22] G. C. Fox and A. J. G. Hey, Nucl.Phys. **B56**, 386 (1973).
[23] G. Cohen-Tannoudji, P. Salin, and A. Morel, Nuovo Cim. **A55**, 412 (1968).
[24] P. K. Williams, Phys. Rev. **D1**, 1312 (1970).
[25] Fayyazuddin, Riazuddin, and M. Ahmad, Lett. Nuovo Cim. **4S1**, 633 (1970), [Lett. Nuovo Cim.4,633(1970)].
[26] M. Guidal, J. M. Laget, and M. Vanderhaeghen, Nucl. Phys. **A627**, 645 (1997).
[27] A. Boyarski, F. Bulos, W. Busza, R. E. Diebold, S. D. Ecklund, G. E. Fischer, J. R. Rees, and B. Richter, Phys.Rev.Lett. **20**, 300 (1968).
[28] D. J. Quinn, J. P. Rutherfoord, M. A. Shupe, D. Sherden, R. Siemann, and C. K. Sinclair, Phys. Rev. **D20**, 1553 (1979).
[29] B. List (H1), in *Proceedings, 17th International Workshop on Deep-Inelastic Scattering and Related Subjects (DIS 2009): Madrid, Spain, April 26-30, 2009* (2009) arXiv:0906.4945 [hep-ex] .
[30] A. Boyarski, R. E. Diebold, S. D. Ecklund, G. E. Fischer, Y. Murata, B. Richter, and W. S. C. Williams, Phys.Rev.Lett. **22**, 148 (1969).
[31] K. O. et al. (Particle Data Group), Chin. Phys. C **38**, 090001 (2014).
[32] S. Bellucci, J. Gasser, and M. E. Sainio, Nucl.Phys. **B423**, 80 (1994), [Erratum: Nucl. Phys.B431,413(1994)], arXiv:hep-ph/9401206 [hep-ph] .
[33] S.-i. Nam and B.-G. Yu, Phys. Rev. **C84**, 025203 (2011), arXiv:1105.1447 [hep-ph] .
[34] T. Sato and T. S. H. Lee, Phys.Rev. **C54**, 2660 (1996), arXiv:nucl-th/9606009 [nucl-th] .
[35] J. D. Jackson and H. Pilkuhn, Nuovo Cim. **33**, 906 (1964).